Exfoliation corrosion behavior of 7050-T6 aluminum alloy treated with various quench transfer time

Feng-xuan SONG, Xin-ming ZHANG, Sheng-dan LIU, Qi TAN, Dong-feng LI

School of Materials Science and Engineering, Central South University, Changsha 410083, China

Abstract: The exfoliation corrosion (EFC) behavior of 7050-T6 aluminum alloy treated with various quench transfer time after solution heat treatment was investigated by standard EFC immersion tests, strength loss measurements after EFC tests and electrochemical impedance spectroscope (EIS) technique. The results showed that EFC resistance of the alloy decreased with increasing quench transfer time. Backscattered electron scanning electron microscope (SEM) together with transmission electron microscope (TEM) observations revealed that the coverage ratio and microstructure of precipitates at grain boundary area are the most important factors which influence the EFC susceptibility of the alloy, while precipitate-free zone (PFZ) near grain boundary has no or only a minor effect on it. In addition, galvanostatic measurements of the alloy present a good correlation between EFC resistance and transients in potential. The cumulated number of transients in potential can be used to evaluate EFC resistance of the alloy.

Key words: 7050-T6 aluminum alloy; thick plate; exfoliation corrosion; quench transfer time; electrochemistry

1 Introduction

7xxx series aluminum alloys have been widely used as structural materials in the modern aviation industry because of their high strength and low density [1,2]. However, these alloys in some tempers are sensitive to localized corrosion such as pitting, intergranular corrosion (IGC), exfoliation corrosion (EFC) and stress corrosion cracking (SCC) [3]. To increase the corrosion resistance, grain structure including grain-boundary precipitates (GBPs) or grain-boundary segregation should be modified. For example, the corrosion resistance of the 7xxx series aluminum alloys can be improved by over-aging (T7) treatment [4,5] or retrogression and re-aging (RRA) treatment [6,7], owing to GBPs coarsening and discontinuous distribution.

Quenching is the most critical step in the sequence of heat-treating operations, because inadequate quenching often results in drop in the mechanical properties and intergranular corrosion resistance after aging [8]. During slow rate quenching, some type of precipitation will occur necessarily on the grain boundaries and can promote the growth of GBPs in the following aging process. As a result, the GBPs of the slowly quenched alloys become coarse and discontinuous. Slow quenching, therefore, should improve the IGC resistances of the alloys according to the above introduction. However, this is in contrast to the general opinion that slow quenching is detrimental to IGC resistance of the 7xxx series aluminum alloys [8]. To solve this question, the effect of quenching process on the microstructure and corrosion resistance of the 7xxx series aluminum alloys needs to be studied further.

Quench transfer time, namely delay during quenching, is an important quenching parameter in industrial production. YOU et al [9] studied the influence of quench transfer time on the mechanical properties of the 7055 alloy. They found that the size and distance of the precipitates on the grain boundary increased with prolonging transfer time, and the strength and elongation decreased slowly with the transfer time increasing within 20 s. In order to obtain a good combination of high strength and low susceptibility to corrosion, the effect of quench transfer time on the properties of 7xxx series aluminum alloys should be evaluated by its corrosion resistance.

Exfoliation corrosion is deteriorating significantly

to the serve life and safety of 7xxx series aluminum alloys. It happens usually on the plates presenting elongated grains and lifts out the material's surface. In this work, the effects of various quench transfer time on the microstructural evolution and exfoliation corrosion behavior in the 7050-T6 aluminum alloy have been investigated. The use of complementary techniques (galvanostatic polarization and electrochemical impedance spectroscopes, scanning and transmission electron microscopes) enables to better understand the relationship between the corrosion behavior and microstructure of the alloys. In addition, the galvanostatic measurement technique enables to relate the EFC resistance to the current and potential transients of the electrochemical measurements.

2 Experimental

2.1 Specimen preparation

The material tested was a hot rolled plate of 7050 aluminum alloy with a thickness of 80 mm, whose composition is 6.06% Zn, 2.20% Mg, 2.12% Cu, 0.11% Zr, 0.08% Fe, 0.04% Si, and balance Al (mass fraction). Samples with a thickness of 2.5 mm were cut from an area near the $S/4$ (S is the plate thickness) of the plate. Solution treatment was carried out in a salt bath at 473 ºC for 1 h. All samples were then taken out from the salt bath, and held for different period in air followed by room temperature water quench. The resident time in air was 2, 16, 45, 120 and 240 s, respectively. Timing was from the emergence of the first corner of a specimen from the salt bath until immersion of the last corner of a specimen in the water quench tank. Aging treatments for as-quenched samples were immediately carried out at 121 ºC for 24 h (T6).

2.2 Microstructure examination

The morphology of the precipitates near grain boundary in the alloys treated with different quench transfer time was examined on Sirion 200 scanning electron microscope (SEM). The morphology and composition analysis of GBPs were studied by FEI TecnaiG^2 20 transmission electron microscope (TEM) together with EDS, operated at 200 kV. Thin foils for TEM observation were made by twin-jet electropolishing, using a mixture solution of 20% nitric acid (14 mol/L) and 80% methanol (0.791−0.793 g/cm^3) cooled to −35 ºC with liquid nitrogen and at 15 V. The size and distribution of GBPs in the typical TEM micrographs were analyzed using imagine pro-plus software. The longest diameter was used as a measure of the size of the plate-shaped particles. For EDS analysis of GBPs, each data point was the arithmetic mean of at least 10 measured GBPs at 3 different grain boundaries. Since each EDS analysis involves Al element, and its content is

approximately identical, the measurement for Cu and Zn content is little affected by the Al content in the matrix [10].

2.3 Corrosion behavior testing

The accelerated exfoliation corrosion (EXCO) test and classification were performed according to the standard EXCO test as described in ASTM G34-01 [11]. The test solution was 4.0 mol/L NaCl + 0.5 mol/L KNO$_3$ + 0.1 mol/L HNO$_3$, and the solution temperature was maintained at 25 ºC. The strength loss percentage after EFC tests was obtained by measuring the tensile property of the un-corroded specimens and specimens suffering from EFC, respectively. The ambient temperature tensile property tests were carried out on CSS-44100 electronic universal testing machine at a tensile velocity of 2 mm/min. The fractured surfaces were characterized by SEM.

Electrochemical impedance spectroscopy (EIS) tests were carried out at the open-circuit potential in the frequency ranging from 0.01 Hz to 100 KHz, using a 5 mV AC signal. A standard three-electrode system, consisting of a saturated calomel electrode as reference electrode, a Pt foil as counter electrode, and the alloy being studied as the working electrode, was connected to CHI 660C Electrochemical Workstation, a product of Shanghai Huachen Instruments Ltd. (Songhua River Road 251 Magnolia Green Square, Shanghai, China). Galvanostatic measurements were tested in a solution of 1 mol/L NaCl + 0.25 mol/L NaNO$_3$, supplemented by 0.033 mol/L AlCl$_3$ in order to buffer the variation of Al^{3+} cations and to hold the pH stable at 3.2, using a 2.5 mA current (I_G) [12].

3 Results and discussion

3.1 Microstructures

The SEM images showing precipitates near the grain boundaries in the 7150-T6 alloys treated with different quench transfer time are shown in Fig. 1. It is noticeable that the grain boundary coverage ratio by the precipitates increases with prolonging quench transfer time. For the quick quench sample, only some large bright particles can be clearly seen (Fig. 1(a)). These are mainly the remnant S-Al$_2$CuMg phase which has not been completely dissolved into the Al matrix during solution heat treatment. With increasing quench transfer time to 45 s, a large number of GBPs with their length less than 10 μm and a large grain structure can be clearly observed (Fig. 1(b)). This suggests that some second phases precipitate on high-angle grain boundaries during transferring to quench, which bring out the recrystallized grain shapes. When prolonging transfer time to 120 s, both the amount and size of GBPs increase remarkably, indicating a higher grain boundary coverage ratio by the
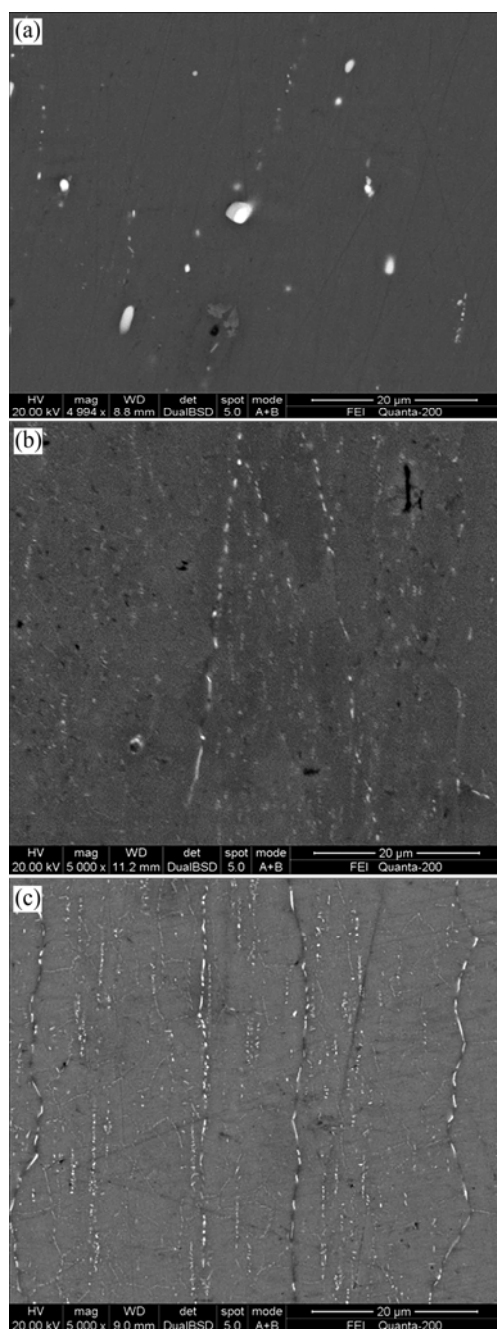
Fig. 1 Backscattered electron SEM images showing grain and sub-grain boundary precipitates in 7050-T6 alloys treated with different transfer time: (a) 2 s; (b) 45 s; (c) 120 s

precipitates compared with the other two conditions (Fig. 1(c)). Specially, a finer grain structure can be seen in Fig. 1(c), owing to more precipitates on sub-grain boundaries. Therefore, it can be inferred that the precipitation temperature range of GBPs during quenching is different on grain boundaries and sub-grain boundaries, which is in line with conclusions of GODARD et al [13].

Figure 2 shows the typical microstructures of 7150-T6 alloy treated with different transfer time by TEM observations. For the sample with transfer time of

2 s, the fine dispersed precipitates with high density can be observed in the matrix (Fig. 2(b)), while GBPs distribute uniformly along the grain boundaries with narrow precipitate free zone (PFZ) (Fig. 2(a)). In addition, it can be seen in Fig. 2(b) that the strengthening particles within the grains are mainly metastable η' ($MgZn_2$) particles. When prolonging transfer time to 45 s, some coarser precipitates mainly equilibrium-state η ($MgZn_2$) particles can be seen (Fig. 2(d)), whereas the size of GBPs and the width of PFZ become larger (Fig. 2(c)). When the transfer time increased to 120 s, the size of GBPs and the width of PFZ are significantly increased (Fig. 2(e)), while a large number of coarser η phase particles precipitate within the grains, even a considerable number of η phase particles appear on Al_3Zr particles because of the core of heterogeneous nucleation (Fig. 2(f)).

The copper content, the size of GBPs, and the width of PFZ in 7050-T6 alloy treated with different transfer time are listed in Table 1. Obviously, the GBPs coarsen and the PFZ becomes wider with the quench transfer time prolonging. The composition of GBPs, however, increases slightly. This relates to the decrease of vacancy and dislocation content in solid solution, which reduces the drive force for alloying elements to diffuse [14]. During transferring, the temperature of the as-solution-treated alloys decreases rapidly, leading to the preferential precipitation of η phase on grain boundaries and dislocations where are highly active [8]. These η phases can act as heterogeneous nucleation sites in the following aging heat treatment. As a result, the size and space of GBPs and the PFZ width all become larger with transfer time prolonging. Note that, the copper content of GBPs increased slightly when transfer time was prolonged. The reason may be that slow quenching can maintain a relatively high material temperature for several minutes (within 4 min for a sheet of 2.5 mm in thickness), although the material temperature reduces continuously during transferring. This is beneficial for copper element to diffuse into the precipitates near grain boundaries. Actually, we have no solid proof to support this hypothesis and it needs to research further in future.

3.2 Exfoliation corrosion evaluations

The EFC behaviors of 7050-T6 alloys treated with various quench transfer time were firstly evaluated by the standard EXCO tests in a more aggressive medium according to ASTM G34-01, and the evolution of the EXCO ratings with immersion time of the alloys is shown in Fig. 3. It can be seen that EXCO resistance decreased with quench transfer time prolonging, and the EXCO rating after 48 h immersion degraded from EC in the immediate quenching condition (transfer time ≤2 s) to ED in the air cooling condition (transfer time ≥240 s).
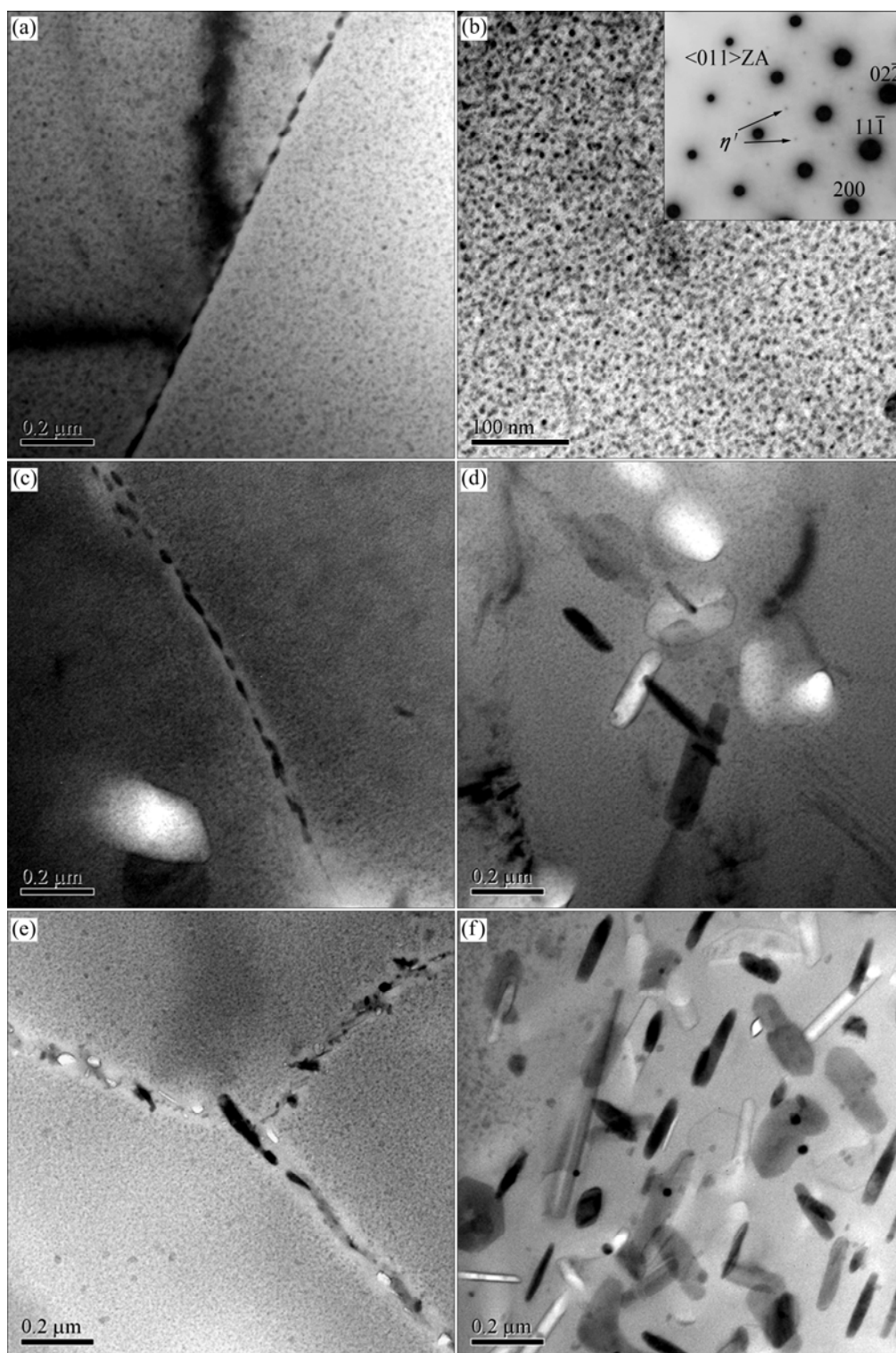
Fig. 2 TEM images of 7050-T6 alloys treated with different transfer time: (a, b) 2 s; (c, d) 45 s; (e, f) 120 s

Table 1 Summary of data showing grain-boundary precipitates size, copper content, and precipitate-free zone width in 7050 alloy treated for different transfer time

| Transfer time/s	GBP size/nm	PFZ width/nm	Zn content in GBP/%	Cu content in GBP/%
45	70 ± 10	60 ± 10	3.8 ± 0.1	2.3 ± 0.2
120	180 ± 20	190 ± 15	3.4 ± 0.5	3.7 ± 0.1
240	195 ± 10	200 ± 15	3.2 ± 0.1	4.1 ± 0.1

For the sample with 16 s transfer time, the EXCO rating after 48 h immersion had almost no change compared with the fast quenched alloys at least by visual evaluation based on corrosion morphologies. Similarly, it is difficult to determine the corrosion difference between the alloys treated with 120 and 240 s transfer time, both which developed a more bad EXCO rating characterizing a severe lift-out of alloy surfaces (ED). Although it is difficult to determine the corrosion difference among all the samples by EXCO rating evaluation, it can still be inferred that the transfer time should be confined in 16 s in order to avoid an apparent degradation of the EFC resistance in this alloy based on the evolution of the EXCO ratings in Fig. 3.
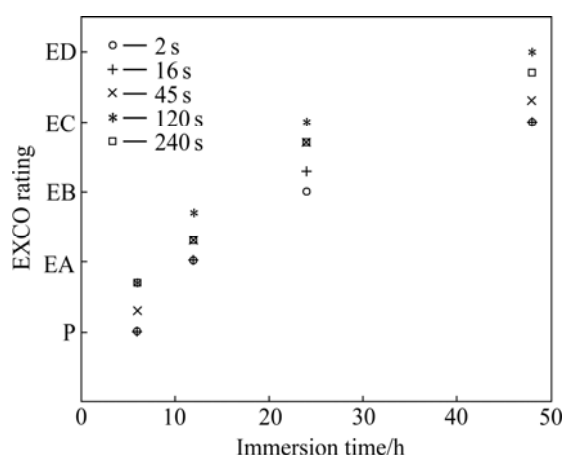
Fig. 3 Evolution of EXCO rating as function of immersion time for 7050-T6 alloys treated with different transfer time according to ASTM G34-01

In order to give quantitative support to morphology descriptions and better presentation about the EFC susceptibilities, yield strength and its loss after EFC of the 7050-T6 alloys were measured, and the results are shown in Fig. 4. Obviously, both the yield strength and its loss decreased with the transfer time prolonging. The strong relationship between the strength loss and quench transfer time demonstrates that the EFC susceptibility increases with prolonging quench transfer time. This is consistent with the coverage ratio of GBPs as referred to above. It is therefore reasonable to conclude that the high EFC susceptibility of the slowly quenched alloys is exactly attributable to the coverage ratio of GBPs (herein η phase). In addition, PFZ has no influence on the corrosion resistance of the alloys or plays a minor role on it, because the PFZ width has grown to an enough large size to act as a separate integrity according to Ref. [15]. But the yield strength loss after EFC of 240 s transfer time sample almost did not decrease compared with that of the 120 s transfer time sample. Indeed, the increase of copper content in the sample treated with 240 s transfer

time will improve the corrosion resistance of it, but the change is so little that its effect can be neglected here. On the other hand, the copper content, neighbor space and coverage ratio at grain boundaries of GBPs are the most important factors influencing the corrosion resistance of the 7050-T6 alloy.
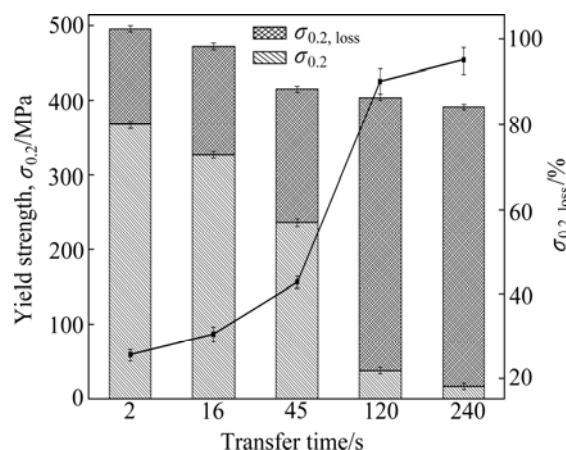

Fig. 4 Yield strength and strength loss after EFC tests of 7050-T6 alloys treated with different transfer time

Figure 5 gives the typical fracture surfaces of the samples with different quench transfer time after EFC attack. The fractured surface of the sample with transfer time of 2 s exhibits mostly transgranular failure, characterized by dimples. In contrast, the fractured surface of the sample with transfer time of 120 s is dominated by intergranular fracture, and some large cracks and cleavage facets can be observed on the fractured surface. The fracture mode of the sample with transfer time of 45 s is a multiple fracture. The fractured surface of this sample indicates a prevailing of transgranular fracture and there are some regions where some small dimples are also observed on the fractured surface. These observations can provide further evidence for EFC resistance decreasing with the increase of quench transfer time.
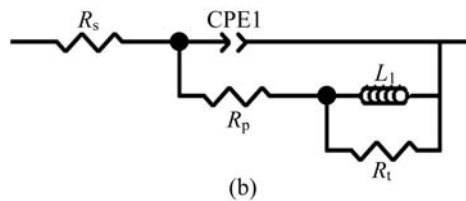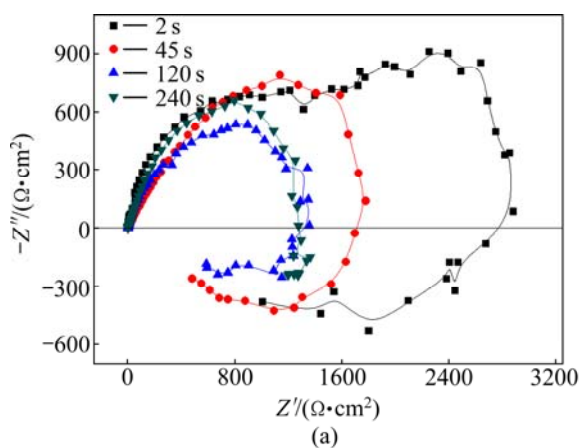
3.3 Electrochemical tests

Figure 6 shows EIS curves of the 7050-T6 alloys treated for different quench transfer time. Nyquist plots in all conditions consist of a high-frequency capacitance arc and a low-frequency induce arc. The radius of capacitance arc decreased with quench transfer time prolonging. This is an indicator of a process under activation control and attacks appearing on the surface of the electrode [16]. The meaning of the inductance, however, is not clear now. To compare the corrosion behavior for different conditions, EIS parameters were obtained by the ZView software and are listed in Table 2. The results show that the solution resistance (R_s) values
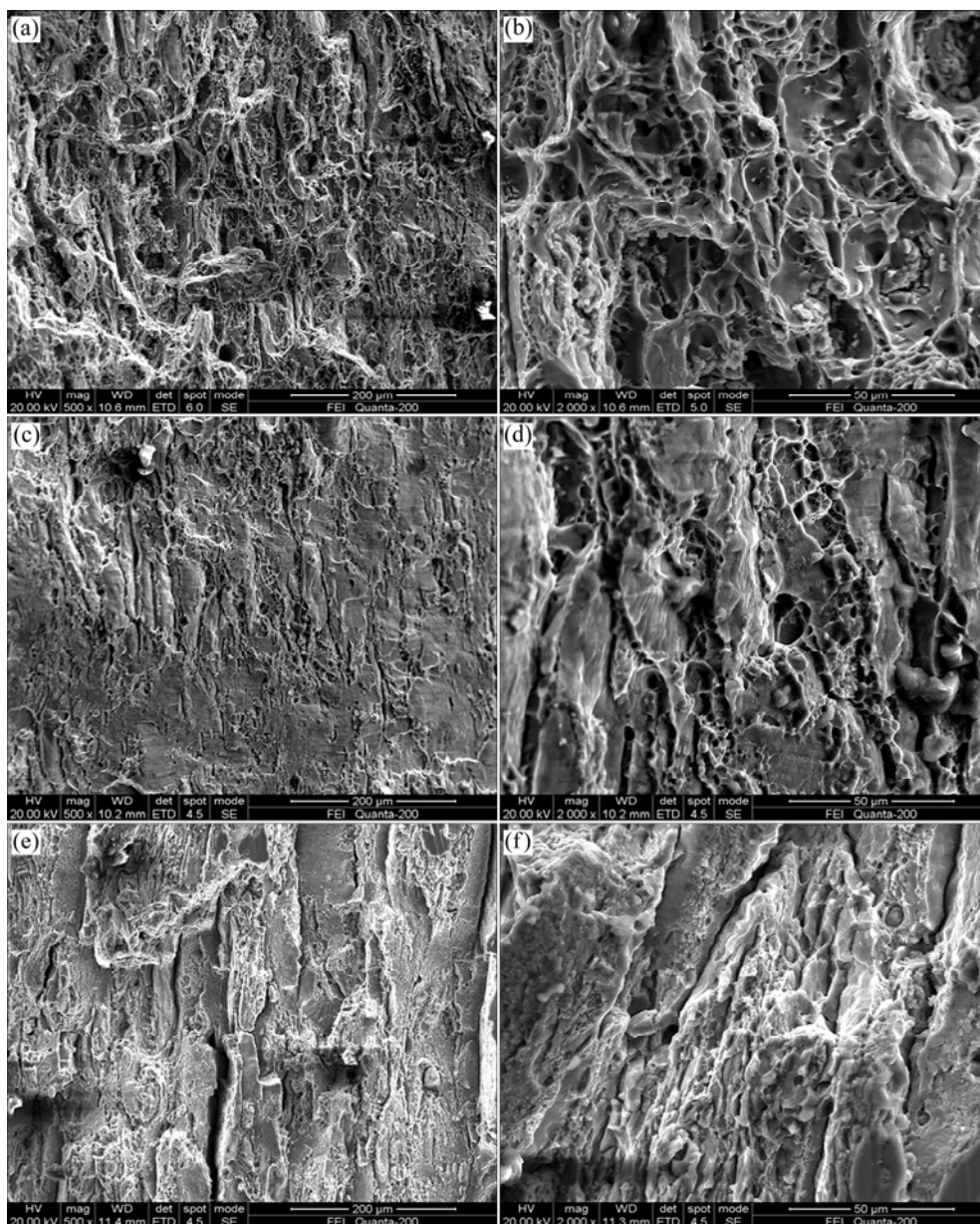
Fig. 5 Fracture surfaces after EFC tests of 7050-T6 alloys treated with different transfer time: (a, b) 2 s; (c, d) 45 s; (e, f) 120 s

Fig. 6 Typical Nyquist plots in 3.5% NaCl solution for 7050-T6 alloys treated with different quench transfer time (a) and corresponding equivalent circuit (b)

Table 2 Electrochemical parameters obtained by fitting analysis of Nyquist plots in Fig. 6

Transfer time/s	$R_s/(\Omega \cdot cm^2)$	$R_p/(\Omega \cdot cm^2)$	$R_t/(\Omega \cdot cm^2)$
2	2.681	1786	2210
45	2.171	606.7	1676
120	3.744	628.9	740
240	3.825	630.1	733

Transfer time/s	CPE-T/(F·cm^{-2})	n	$L/(H \cdot cm^2)$
2	4.155×10^{-5}	0.8391	5374
45	3.225×10^{-4}	0.6012	3740
120	1.421×10^{-4}	0.7749	3107
240	1.496×10^{-4}	0.7451	3479

Fig. 7 Evolution of potential with time during galvanostatic test for 7050-T6 alloys treated with different quench transfer time

Fig. 8 Variation of cumulated number of transients in 12 h of galvanostatic test for 7050-T6 alloys with quench transfer time

of the alloys vary negligibly, while the polarization resistance (R_p) and charge transfer resistance (R_t) values vary more significantly with prolonging the quench transfer time. The value of R_t is inversely proportional to the value of corrosion current density (J_{corr}) in all instances [17]. Therefore, the corrosion resistance of the alloys decreased with prolonging quench transfer time because of the increase of R_t values, which is consistent with the yield strength loss. In the equivalent circuit (Fig. 6(b)), capacitance was mathematically modeled using a constant phase element (CPE) in order to obtain a better simulation between the model and the experimental data. CPE represents an imperfect/leaking capacitor, and means an ideal capacitance, a resistance and a Warburg impedance when n=1, 0, and −1, respectively [18]. In addition, the value of inductance decreased with prolonging transfer time, and were proportional to the corrosion resistance of the alloys.

Galvanostatic measurements can be used to more accurately evaluate the EFC difference of differently heat-treated alloys according to the work by MARLAUD et al [12,19]. The evolution of potential fluctuations with immersion time in a solution of 1 mol/L NaCl + 0.25 mol/L NaNO$_3$ and the variation of cumulated number of transients in 12 h of galvanostatic test of the 7050-T6 alloys as a function of quench transfer time are shown in Figs. 7 and 8, respectively. For the samples treated with 240 s quench transfer time, a large number of potential fluctuations were recorded, typically characterized by a sharp drop in potential followed by a gradual return to a steady state value. With the decrease of transfer time, both the number and amplitude of potential fluctuations reduced, implying a good relationship between the potential transient and individual EFC event. To find out some relations, a 2 mV threshold was used to detect the cumulated number of transients in 12 h of galvanostatic test for all the 7050-T6 alloys. Immediately, it is obvious
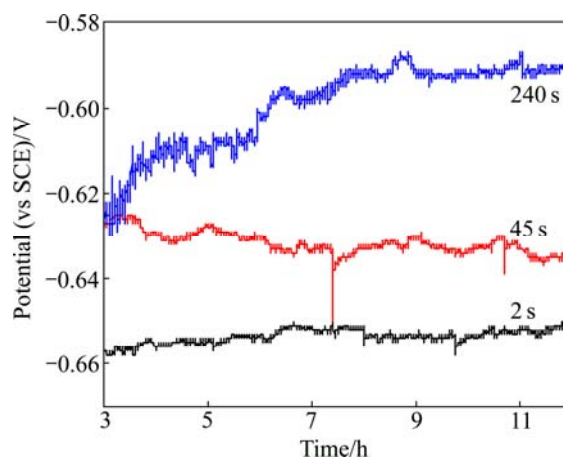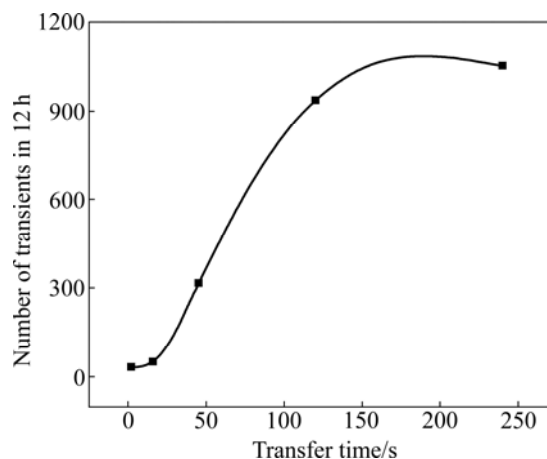
to see that the cumulated number of transients increases with prolonging quench transfer time, which is in good agreement with the EFC susceptibility. It is very useful to evaluate the EFC resistance of the alloys, especially when the visual determination is difficult.

4 Conclusions

1) The EFC resistance of the 7050-T6 aluminum alloy decreases with prolonging quench transfer time. In order to maintain a high resistance to EFC, the transfer time should be controlled within 16 s.

2) The coverage ratio and microstructure (including size, the nearest neighbor space and chemical composition) of GBPs are the most important factors which influence the corrosion resistance of the alloys, while PFZ has no or a minor influence on it.

3) The potential fluctuations during galvanostatic tests are exactly related to some EFC events, and the cumulated number of transients in potential can be used to evaluate EFC resistance of the alloys.

References

[1] REFEDIOS K H. Aluminium structures used in aerospace—Status and prospects [J]. Material Science Forum, 1997, 242: 11−42.

[2] CHEN Song-yi, CHEN Kang-hua, JIA Le, PENG Guo-sheng. Effect of hot deformation conditions on grain structure and properties of 7085 aluminum alloy [J]. Transactions of Nonferrous Metals Society of China, 2013, 23(2): 329−334.

[3] LI Jin-feng, PENG Zhuo-wei, LI Chao-xing, JIA Zhi-qiang, CHEN Wen-jing, ZHENG Zi-qiao. Mechanical properties, corrosion behaviors and microstructures of 7075 aluminium alloy with various aging treatments [J]. Transactions of Nonferrous Metals Society of China, 2008, 18(4): 755−762.

[4] WILLIAMS J C, STARKE E A Jr. Progress in structural materials for aerospace systems [J]. Acta Materialia, 2003, 51(19): 5775−5799.

[5] WLOKA J, HACK T, VIRTANEN S. Influence of temper and surface condition on the exfoliation behaviour of high strength Al–Zn–Mg–Cu alloys [J]. Corrosion Science, 2007, 49(3): 1437−1449.

[6] CINA B, GAN R. Reducing the susceptibility of alloys, particularly aluminium alloys, to stress corrosion cracking: USA, 3856584 [P]. 1974.

[7] LI Guo-feng, ZHANG Xin-ming, LI Peng-hui, YOU Jiang-hai. Effects of retrogression heating rate on microstructures and mechanical properties of aluminum alloy 7050 [J]. Transactions of Nonferrous Metals Society of China, 2010, 20(6): 935−941.

[8] ASM International. ASM handbook: Heat treating [M]. Volume 4. Metals Park, Ohio: American Society for Metals, 1991.

[9] YOU Jiang-hai, LIU Sheng-dan, ZHANG Xin-ming, ZHANG Xiao-yan. Influence of quench transfer time on microstructure and mechanical properties of 7055 aluminum alloy [J]. Journal of Central South University, 2008, 15(2): 153−158.

[10] PENG G S, CHEN K H, CHEN S Y, FANG H C. Influence of repetitious-RRA treatment on the strength and SCC resistance of Al–Zn–Mg–Cu alloy [J]. Materials Science and Engineering A, 2011, 528(12): 4014−4018.

[11] ASTM G34-01. Standard test method for exfoliation corrosion susceptibility in 2xxx and 7xxx series aluminum alloys (EXCO test) [S].

[12] MARLAUD T, MALKI B, DESCHAMPS A, BAROUX B. Electrochemical aspects of exfoliation corrosion of aluminium alloys: The effects of heat treatment [J]. Corrosion Science, 2011, 53(4): 1394−1400.

[13] GODARD D, ARCHAMBAULT P, AEBY-GAUTIER E, LAPASSET G. Precipitation sequences during quenching of the AA 7010 alloy [J]. Acta Materialia, 2002, 50(9): 2319−2329.

[14] THOMPSON D S, SUBRAMANYA B S, LEVY S A. Quench rate effects in Al–Zn–Mg–Cu alloys [J]. Metallurgical Transactions, 1971, 2(4): 1149−1160.

[15] RALSTON K, BIRBILIS N, WEYLAND M, HUTCHINSON C. The effect of precipitate size on the yield strength-pitting corrosion correlation in Al–Cu–Mg alloys [J]. Acta Materialia, 2010, 58(18): 5941−5948.

[16] DENG Y, YIN Z M, ZHAO K, DUAN J Q, HU J, HE Z B. Effects of Sc and Zr microalloying additions and aging time at 120 °C on the corrosion behaviour of an Al–Zn–Mg alloy [J]. Corrosion Science, 2012, 65: 288−298.

[17] CAO Fa-he. Electrochemical study on the localized corrosion behavior of high strength aircraft aluminum alloys [D]. Hangzhou: Zhejiang University, 2005. (in Chinese)

[18] LI Jin-feng, CHEN Wen-jing, ZHAO Xu-shan, REN Wen-da, ZHENG Zi-qiao. Corrosion behavior of 2195 and 1420 Al-Li alloys in neutral 3.5% NaCl solution under tensile stress [J]. Transactions of Nonferrous Metals Society of China, 2006, 16(5): 1171−1177.

[19] MARLAUD T, MALKI B, HENON C, DESCHAMPS A, BAROUX B. Relationship between alloy composition, microstructure and exfoliation corrosion in Al–Zn–Mg–Cu alloys [J]. Corrosion Science, 2011, 53(10): 3139−3149.

不同淬火转移时间处理的 7050-T6 铝合金剥落腐蚀行为

宋丰轩，张新明，刘胜胆，谈 琦，李东锋

中南大学 材料科学与工程学院，长沙 410083

摘 要：采用标准的剥落腐蚀浸蚀实验、剥落腐蚀后样品的强度损失测量以及电化学阻抗谱等技术，对固溶后经不同淬火转移时间处理的 7050-T6 态样品的剥落腐蚀行为进行研究。结果表明，7050-T6 铝合金的抗剥落腐蚀性能随着淬火转移时间的延长而减小。背散射电子扫描连同透射电镜观察揭示，影响合金腐蚀性能的最主要因素是晶界的析出相覆盖率和析出相的微观组织，而晶界附近的贫溶质区对其不产生影响或影响较小。通过对合金进行静电势扫描发现，合金的剥落腐蚀敏感性与瞬态电势之间有很好的对应关系，即可以测试瞬态电势变化的数量来表征材料的剥蚀性能。

关键词：7050-T76 铝合金；厚板；剥落腐蚀；淬火转移时间；电化学

(Edited by Sai-qian YUAN)